J. Appl. Comput. Mech., 8(4) (2022) 1324-1331
DOI: 10.22055/jacm.2022.39877.3479

ISSN: 2383-4536
jacm.scu.ac.ir

Shahid Chamran
University of Ahvaz

Journal of
Applied and Computational Mechanics

Research Paper

Multi-objective Optimal Design of Carbon and Glass Reinforced Hybrid Composites under Flexural Loading

Chensong Dong

School of Civil and Mechanical Engineering, Curtin University, GPO Box U1987, Perth WA 6845, Australia

Received January 28 2022; Revised March 27 2022; Accepted for publication April 02 2022.
Corresponding author: C. Dong (c.dong@curtin.edu.au)

Abstract. Hybrid composites reinforced by two types of fibres e.g., carbon and glass have been widely researched. These two types of fibres are distinct in density and cost. An optimisation study on the carbon and glass fibre reinforced hybrid composite in three-point bending is presented in this paper. Both unidirectional and multi-directional hybrid composites are studied. The objectives are minimising the cost and weight with the flexural strength being the constraint. The three-point bending is simulated by a Finite Element Analysis based model, and optimisation is done with non-dominated sorting GA-II (NSGA-II). This optimisation approach can be extended to hybrid composites reinforced by other types of fibres.

Keywords: Composite; hybrid; flexural; optimisation.

1. Introduction

Hybrid composites comprising two or more types of fibre have received significant attention in engineering design because of the potential of achieving balanced properties. One common type of hybrid composite is the carbon and glass fibre reinforced hybrid composite. Previous research on this material suggested that the flexural strength could be improved via hybridisation [1-5]. The main reason is that glass fibre has higher strain-to-failure than carbon fibre, and consequently, the strain-to-failure is increased due to the inclusion of glass fibre [6]. Rajpurohit et al. [7] showed positive hybrid effects in tension and compression. Zhang et al. [8] showed the carbon/glass interlayer hybrid composite had improved low velocity impact performance. The existence of hybrid effect can be potentially useful for achieving a balanced cost and weight optimal composite material. It is shown carbon and glass fibre reinforced hybrid composites have been used in windsurf boards and wind turbine blades [9].

A composite laminate usually comprises several laminas or plies. In the design process, the fibre type, fibre orientation and fibre volume fraction of each ply need to be carefully selected to meet the design requirements. Optimisation of composites has been reviewed by Ghiasi et al. [10-11] and Nikbakt et al. [12]. It is shown from these review studies that the focus of optimisation is the stacking sequence. Not much has been done for the hybrid composites.

Two important design objectives are weight and cost minimisation. Carbon fibre is more expensive but lighter than glass fibre. For the carbon and glass fibre reinforced hybrid composite, weight and cost are two conflicting requirements and thus trade-off needs to be made. An optimisation problem to minimise the cost and weight of composites is called a multi-objective optimisation problem.

In classical multi-objective optimisation methods, the objectives are transformed into a single objective using *a priori* methods and preference-based strategies [13]. These methods have been used in the design optimisation of composites [14-16]. The disadvantage of these methods is choosing a reliable and accurate preference of the objectives requires higher-level information which may not be available during the initial stages of the design process [17]. Alternatively, *a posteriori* methods can be used, from which a set of trade-off solutions, which is known as a Pareto set, is generated. The final design decision is made after additional evaluation and comparison of the Pareto set. A multi-objective optimization evolutionary algorithm (MOEA), which is classified as an *a posteriori* method, can be utilized to produce a set of Pareto optimal sets in a single simulation and hence improve the solutions in several evolutions without considering any preference of objectives. MOEAs achieve Pareto optimal sets in a single run and through evolution of a random initial population in several iterations called generations. Several MOEA methods are available, including strength Pareto evolutionary algorithm (SPEA-II) [18], Pareto archived evolutionary strategy (PAES) [19] and the non-dominated sorting GA (NSGA) [20]. A modified version of the NSGA, known as NSGA-II, is one of the most popular MOEAs due to its simplicity and efficiency [20]. NSGA-II has been used in our previous research to minimise the cost and weight of unidirectional [21-22] and multidirectional [23-24] hybrid composites. It is shown from these studies that the positive hybrid effects help to reduce the cost and weight of the composite. These studies, however, were based on simple Classical Lamination Theory (CLT) and did not truly simulate the flexural behaviour of the hybrid composite in three-point bend test. In a more recent study, the flexural behaviour of hybrid composites in three-point bend test was simulated by Finite Element Analysis (FEA) [25]. It has been shown that NSGA-II and FEA could be coupled [26] for the optimisation of a wind turbine blade for a specific 15 kW turbine with the mass as one of the objectives.

Published online: April 12 2022

Table 1. Selected properties of fibres and resin.

Material	Tensile Modulus (GPa)	Tensile Strength (MPa)	Density (kg/m^3)	Cost ($/litre) [e]
High strength carbon fibre [a]	230	4900	1800	151.2
E glass fibre [b]	72	3450	2580	10.8
S-2 glass [c]	86.9	4890	2460	103.3
High performance epoxy matrix [d]	3.1	69.6	1090	26.2

[a] T700S® 12K, Toray Industries, Inc., Tokyo, Japan
[b] E glass SE 2350 single-end roving, Owens Corning, Toledo, OH, USA
[c] S-2 glass unidirectional Unitex plain weave UT-S500 fibre mat, SP System, Newport, Isle of Wight, UK
[d] Kinetix R240 high performance epoxy resin with H160 hardener at a ratio of 4:1 by weight, ATL Composites Pty Ltd., Australia
[e] All material prices were converted to US$.

In this paper, an optimisation study based on NSGA-II was conducted to achieve the optimal hybrid composite under flexural loading with minimum cost and weight as the objective functions. The three-point bending was chosen because the flexural properties can be improved via hybridisation, while other properties approximately follow the Rule of Mixtures (RoM). The flexural behaviour of hybrid composites was modelled by FEA. Optimisation was done by coupling NSGA-II and FEA-based model. Both the unidirectional and multi-directional hybrid composites were studied.

2. Methodology

In this section, the FEA-based modelling approach and optimisation procedure are presented.

2.1 Materials

In this study, a high strength carbon fibre was chosen to be the carbon fibre, and two types of glass fibres, i.e., E glass and S-2 glass fibres were chosen to be the glass fibre. An epoxy was chosen to be the matrix. Epoxy resins are widely used in composites because of their high strength (tensile, compressive and flexural), good chemical resistance, fatigue resistance, corrosion resistance and electrical resistance [27]. The properties of the fibres and epoxy resin are presented in Table 1 [1].

2.2 Properties of Composites

For each ply, based on the constituent properties and its fibre volume fraction, the ply properties, including the longitudinal modulus E_{11}, the transverse moduli E_{22} and E_{33}, and the shear moduli G_{12}, G_{13} and G_{23}, are derived by Hashin's model [28]. The strength components of composites were derived, and stress-based failure criteria were employed. When failure occurs in a ply, stiffness degradation factors [29] were used to reduce the stiffness. The stiffness degradation factor was chosen to be 0.9.

The weight of a composite material can be characterised by its density. The density of the hybrid composite reinforced by carbon and glass fibres, ρ_c, can be derived based on RoM as follows:

$$\rho_c = \rho_{fc}V_{fc} + \rho_{fg}V_{fg} + \rho_m V_m \tag{1}$$

where ρ_{fc}, ρ_{fg} and ρ_m are the densities of carbon fibre, glass fibre and the matrix, respectively, and V_{fc}, V_{fg} and V_m are the volume fractions of carbon fibre, glass fibre and the matrix, respectively.

The material cost of the hybrid composite, C_c, is given by

$$C_c = C_{fc}V_{fc} + C_{fg}V_{fg} + C_m V_m \tag{2}$$

where C_{fc}, C_{fg} and C_m are the costs of carbon fibre, glass fibre and the matrix, respectively.

2.3 Model Development

The hybrid composite in this study comprises eight plies and the thickness of each ply is 0.25 mm. The total thickness is 2 mm, the width is 10 mm, and the length is 100 mm. The flexural properties of hybrid composites were evaluated via FEA-based three-point bending simulation in accordance with ASTM D7264 [30]. A unidirectional hybrid composite specimen being supported by two supporters at a span of L and loaded at its mid-span is shown in Fig. 1. The span-to-thickness ratio was chosen to be 32. The composite specimen is loaded in such way that plies 1 and 8 are in tensile and compressive, respectively.

The three-point bending process was simulated by FEA using Ansys Workbench. The hybrid composite is modelled as a shell structure. Since the hybrid composite specimen is modelled as a surface, no free-edge effects and stress concentration between layers. A sufficiently high span-to-thickness ratio is chosen so that the bending stress is dominant and the effect of interlaminar shear stress is minimised. It is shown from our previous research [1-2] that the primary failure mode is the kinking and microbuckling on the compressive side of the specimen under the loading nose. The supporters and the loading nose are modelled as cylindrical solids made of steel. Fixed support is applied to the supporters and a pre-scribed displacement of 7 mm in the negative z direction is applied to the loading nose. Frictional contact is defined between the supporters and the composite specimen, and between the loading nose and the composite specimen. Previous research by the present author [31] shows the contact stress has negligible effect in this case. The dominant failure mode for all similar hybrid composite specimens under three-point bending load is in-plane failure for large span-to-thickness ratios.

Linear static analysis is conducted to obtain the flexural strength at first-ply failure. Upon completion of simulation, the reaction force due to the prescribed displacement is obtained. The maximum failure criterion, which is the ratio of the maximum stress to the failure stress, is also obtained. When the maximum failure criterion is less than 1, no failure occurs, and when the maximum failure criterion is greater than or equal to 1, failure occurs somewhere in the specimen. The failure load is obtained by working out the ratio of the reaction force and maximum failure criterion. The flexural strength is calculated using the failure load by the formula in ASTM D7264. This developed modelling approach was validated against the experimental data [25]. For the full carbon fibre unidirectional composite with 30% fibre volume fraction, the deformation from FEA is shown in Fig. 2.

For the multi-directional hybrid composite, two loading conditions were simulated. In addition to the loading condition above, which is denoted longitudinal, the hybrid composite specimen is also duplicated and rotated by 90°, which is denoted transverse, as shown in Fig. 3. Both specimens have the same layup.

2.4 NSGA-II-Based Optimisation

The developed FEA-based model was applied to conduct optimisation using NSGA-II. It is shown from previous research that the flexural strength of the composite can be improved via hybridisation. The present study aimed to minimise the density and cost of carbon/glass fibre reinforced epoxy hybrid composites subjected to a minimum flexural strength. The flowchart of NSGA-II-based optimisation is shown in Fig. 4.

Optimisation was carried out for two different types of hybrid composites. First, the unidirectional hybrid composites were studied. The hybrid composite specimen comprised eight plies of 0.25 mm thickness. The optimisation problem is formulated as:

$$\text{Min}\begin{cases} C_c \\ \rho_c \end{cases} \qquad \text{s.t. } S_F \geq S_{F0} \tag{3}$$

where S_{F0} is the minimum required flexural strength.

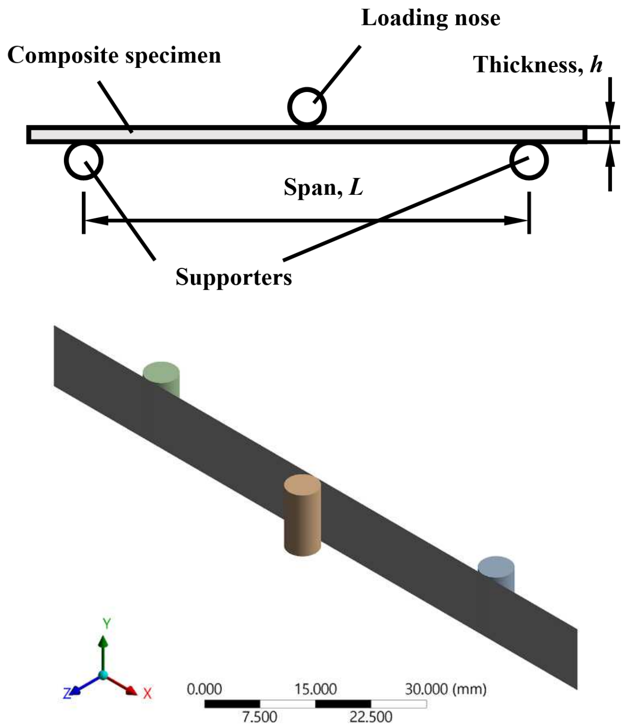

Fig. 1. A unidirectional hybrid composite specimen in three-point bending.

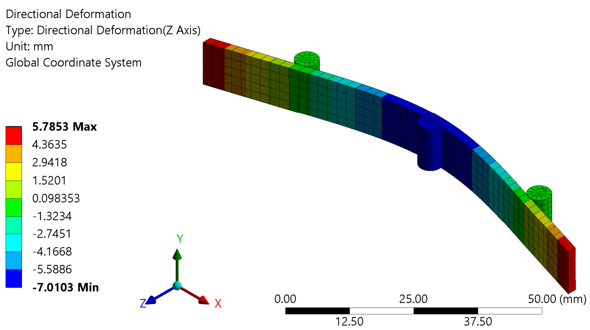

Fig. 2. Deformation from FEA for full carbon fibre unidirectional composite in three-point bending.

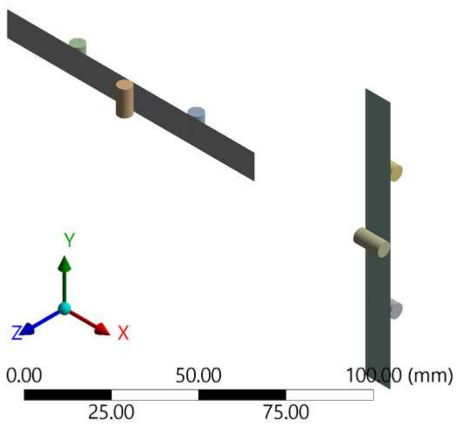

Fig. 3. FEA model for multi-directional hybrid composite in three-point bending.

Table 2. Variables and their ranges of value in optimization.

Variable	Range of value
V_{fc}	[0.3, 0.6]
V_{fg}	[0.3, 0.6]
Ply material	[Carbon/epoxy, glass/epoxy]

The design variables are the fibre volume fractions of carbon/epoxy and glass/epoxy composites, and the fibre type of each ply. The variables and their ranges of value are shown in Table 2.

The optimisation started from a full carbon fibre composite. The number of initial samples was 83 and the number of samples each iteration was 83. Up to 10 candidate points were found from optimisation. Four minimum flexural strengths, 700 MPa, 1000 MPa, 1300 MPa, and 1600 MPa, were chosen.

Secondly, the multi-directional hybrid composites were studied. The composite specimen comprised six plies of 0.25 mm thickness. Both fibre volume fractions were varied between 0.3 and 0.7. The optimisation problem is formulated as:

$$\text{Min}\begin{cases} C_c \\ \rho_c \end{cases} \quad \text{s.t. } S_F \geq S_{F0} \text{ and } S_{FT} \geq S_{F0} \tag{4}$$

where S_{FT} is the flexural strength when transversely loaded.

In addition to the design variables listed in Table 2, the fibre orientation angle of each ply was also included as a design variable. The fibre orientation angle was chosen to be discrete and varied between four levels, i.e. -45°, 0°, 45°, and 90°.

The optimisation also started from a full carbon fibre composite. The number of initial samples was 116 and the number of samples each iteration was 116. Up to 10 candidate points were found from optimisation. Five minimum flexural strengths, 500 MPa, 600 MPa, 700 MPa, 800 MPa, and 900 MPa, were chosen.

3. Results and Discussion

3.1 Unidirectional Hybrid Composites

The NSGA-II-based optimisation converges after 397-614 runs. The Pareto fronts from NSGA-II optimisation for the carbon/E glass and carbon/S-2 glass fibre reinforced unidirectional hybrid composites are shown in Fig. 5. It is shown that the carbon/E glass fibre reinforced hybrid composite in general offers lower material cost but higher weight. When the required flexural strength is 1300 MPa, the carbon/E glass fibre reinforced hybrid composite offers some optimal designs with lower cost compared to the carbon/S-2 glass fibre reinforced hybrid composite, and some of these designs have comparable similar weight as to the carbon/S-2 glass fibre reinforced hybrid composite. When the required flexural strength is 1600 MPa, the carbon/E glass fibre hybrid composite has a much wide range of cost and weight compared to the carbon/S-2 glass fibre reinforced hybrid composite.

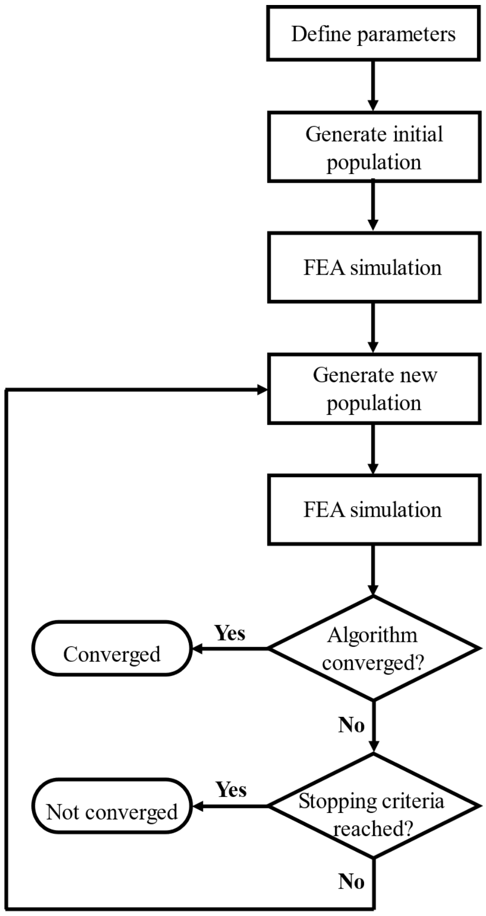

Fig. 4. Flowchart of optimisation based on NSGA-II and FEA.

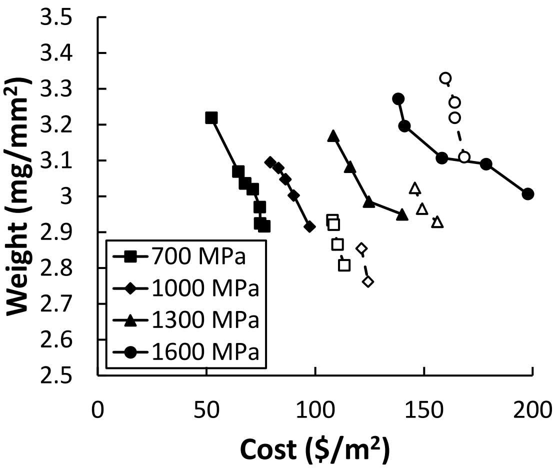

Fig. 5. Pareto fronts from NSGA-II optimisation for carbon/E glass fibre reinforced (filled symbols) and carbon/S-2 glass fibre reinforced (open symbols) unidirectional hybrid composites.

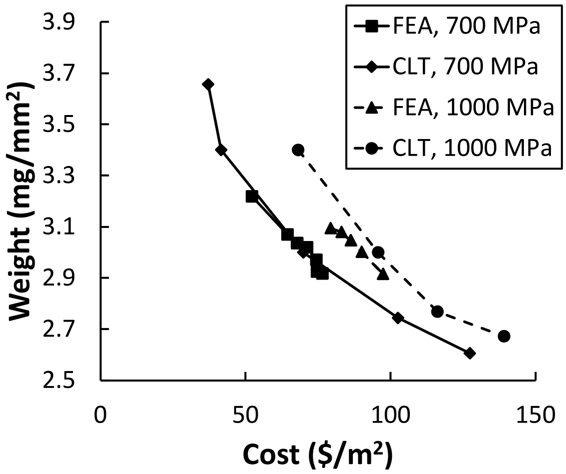

Fig. 6. Pareto fronts from FEA-based optimisation and CLT-based optimisation.

When the required flexural strength is 700 MPa, the results from optimisation are shown in Tables 3 and 4. For the carbon/E glass fibre reinforced hybrid composite, it is shown that E glass/epoxy is mostly chosen to be the material on the compressive side (ply 8). An exception is candidate point 3, which is a sandwich type composite with carbon/epoxy plies being placed on the outside of the composite. For the carbon/S-2 glass fibre reinforced hybrid composite, it is shown that either two or three glass/epoxy plies are placed on the compressive side of the composite.

When the required flexural strength is 1000 MPa, the optimal results are shown in Tables 5 and 6. For the carbon/E glass fibre reinforced hybrid composite, the outermost ply on the tensile side (ply 1) is carbon/epoxy. The outermost ply on the compressive side (ply 8) is mostly glass/epoxy, except for candidate 3, which has carbon/epoxy plies on both the tensile and compressive sides. For the carbon/S-2 glass fibre reinforced hybrid composite, only two candidates have been found. From the results of both the E glass and S-2 glass hybrid composites, two typical layups can be identified. The first typical layup is placing glass/epoxy plies on the compressive side and carbon/epoxy plies on the tensile side. An example is $[0_{2G}/0_{6C}]$ in Table 6. The second typical layup is placing glass/epoxy plies on the tensile side below the mid-plane. These two typical layups can also be combined. For example, $[0_{G}/0_{3C}/0_{3G}/0_{C}]$ in Table 6 reflects this combination. This is in good agreement with a previous study [31].

The flexural strengths of the carbon and S-2 glass fibre reinforced hybrid composite from the FEA predictions are compared with those obtained by CLT from a previous study [31]. As shown in Table 7, FEA gives slightly higher flexural strengths than CLT. In other words, CLT underestimates the flexural strength. The Pareto fronts from FEA-based optimisation and CLT-based optimisation are shown in Fig. 6. Because CLT underestimates the flexural strength, both the cost and weight from FEA-based optimisation are slightly higher than those form FEA-based optimisation.

Table 3. Optimal results for carbon and E glass fibre reinforced unidirectional hybrid composite with minimum flexural strength 700 MPa.

	V_{fc}	V_{fg}	Layup (ply 8 – ply 1)	Flexural strength (MPa)	Cost ($/m²)	Weight (mg/mm²)	Hybrid ratio
1	0.3018	0.3133	$[0_{4G}/0_{C}/0_{G}/0_{2C}]$	706.03	74.66	2.9242	0.6337
2	0.3197	0.3042	$[0_{G}/0_{C}/0_{3G}/0_{C}/0_{G}/0_{C}]$	748.33	76.52	2.9167	0.6132
3	0.3222	0.3466	$[0_{C}/0_{3G}]_{S}$	721.52	64.53	3.0690	0.7634
4	0.3659	0.3250	$[0_{G}/0_{C}/0_{2G}]_{S}$	731.11	67.76	3.0362	0.7271
5	0.3047	0.3372	$[0_{4G}/0_{C}/0_{G}/0_{2C}]$	731.11	67.76	3.0362	0.7271
6	0.3186	0.3768	$[0_{G}/0_{C}/0_{6G}]$	739.57	74.48	2.9703	0.6484
7	0.4165	0.3097	$[0_{G}/0_{C}/0_{2G}]_{S}$	704.61	52.20	3.2191	0.8922

Table 4. Optimal results for carbon and S-2 glass fibre reinforced unidirectional hybrid composite with minimum flexural strength 700 MPa.

	V_{fc}	V_{fg}	Layup (ply 8 – ply 1)	Flexural strength (MPa)	Cost ($/m²)	Weight (mg/mm²)	Hybrid ratio
1	0.3018	0.3065	$[0_{2G}/0_{2C}/0_{3G}/0_{C}]$	879.99	110.23	2.8656	0.6286
2	0.3088	0.3133	$[0_{3G}/0_{C}/0_{2G}/0_{C}/0_{G}]$	704.29	107.93	2.9334	0.7527
3	0.3391	0.3020	$[0_{3G}/0_{C}]_{2}$	795.03	108.52	2.9210	0.7277
4	0.3018	0.3018	$[0_{2G}/0_{2C}]_{2}$	920.49	113.40	2.8078	0.5000

Table 5. Optimal results for carbon and E glass fibre reinforced unidirectional hybrid composite with minimum flexural strength 1000 MPa.

	V_{fc}	V_{fg}	Layup (ply 8 – ply 1)	Flexural strength (MPa)	Cost ($/m²)	Weight (mg/mm²)	Hybrid ratio
1	0.3669	0.3862	$[0_{2G}/0_{2C}/0_{3G}/0_{C}]$	1023.85	79.36	3.0946	0.6369
2	0.4030	0.3674	$[(0_{2G}/0_{C})_{2}/0_{G}/0_{C}]$	1000.18	83.11	3.0789	0.6031
3	0.3977	0.3042	$[0_{2C}/0_{3G}/0_{C}/0_{G}/0_{C}]$	1002.39	97.42	2.9155	0.4334
4	0.3488	0.3857	$[0_{2G}/0_{2C}]_{2}$	1051.95	90.06	3.0023	0.5251
5	0.4319	0.3422	$[0_{2G}/0_{2C}/0_{3G}/0_{C}]$	1077.91	86.31	3.0474	0.5691
6	0.4319	0.3422	$[0_{G}/0_{2C}/0_{4G}/0_{C}]$	1056.54	86.31	3.0474	0.5691

Table 6. Optimal results for carbon and S-2 glass fibre reinforced unidirectional hybrid composite with minimum flexural strength 1000 MPa.

	V_{fc}	V_{fg}	Layup (ply 8 – ply 1)	Flexural strength (MPa)	Cost ($/m²)	Weight (mg/mm²)	Hybrid ratio
1	0.3069	0.3724	$[0_{2G}/0_{6C}]$	1003.49	124.30	2.7619	0.2880
2	0.3632	0.3042	$[0_{G}/0_{3C}/0_{3G}/0_{C}]$	1000.10	121.25	2.8546	0.4558

Table 7. Comparison of flexural strengths from FEA and CLT.

Layup	Flexural strength (MPa)	
	FEA	CLT
$[0]_{10C}$	948	907
$[0_{2G}/0_{8C}]$	1191	1143
$[0_{8C}/0_{2G}]$	856	818
$[0]_{10G}$	946	910
$[0/90]_{5C}$	548	518
$[0_G/90_C/90_G/0_C/0_G]_S$	618	500
$[(0/45/-45/90/0)_C]_S$	552	519
$[0_{2G}/0_{2C}/(90/45/90_2/0_2)_C]$	1159	1108

Table 8. Optimal results for carbon and E glass fibre reinforced unidirectional hybrid composite with minimum flexural strength 1300 MPa.

	V_{fc}	V_{fg}	Layup (ply 8 – ply 1)	Flexural strength (MPa)	Cost ($\$/m^2$)	Weight (mg/mm^2)	Hybrid ratio
1	0.4869	0.3340	$[0_{3C}/0_{3G}/0_{2C}]$	1348.98	124.61	2.9853	0.2916
2	0.5512	0.3427	$[0_{3C}/0_{4G}/0_C]$	1416.34	116.02	3.0820	0.3834
3	0.5001	0.4255	$[0_{2G}/0_{2C}]_2$	1302.43	108.36	3.1690	0.4597
4	0.4812	0.3450	$[0_{3C}/0_G]_S$	1332.43	139.96	2.9495	0.1929

Table 9. Optimal results for carbon and S-2 glass fibre reinforced unidirectional hybrid composite with minimum flexural strength 1300 MPa.

	V_{fc}	V_{fg}	Layup (ply 8 – ply 1)	Flexural strength (MPa)	Cost ($\$/m^2$)	Weight (mg/mm^2)	Hybrid ratio
1	0.4940	0.3379	$[0_{3C}/0_{3G}/0_{2C}]$	1365.83	149.12	2.9656	0.2910
2	0.5404	0.3357	$[0_{2C}/0_G/0_C/0_{3G}/0_C]$	1307.46	145.83	3.0236	0.3832
3	0.4828	0.3422	$[0_{3C}/0_G/0_C/0_G/0_{2C}]$	1325.53	156.12	2.9286	0.1911
4	0.4828	0.3422	$[0_{4C}/0_{2G}/0_{2C}]$	1356.06	156.12	2.9286	0.1911

Table 10. Optimal results for carbon and E glass fibre reinforced unidirectional hybrid composite with minimum flexural strength 1600 MPa.

	V_{fc}	V_{fg}	Layup (ply 8 – ply 1)	Flexural strength (MPa)	Cost ($\$/m^2$)	Weight (mg/mm^2)	Hybrid ratio
1	0.5816	0.4124	$[0_{4C}/0_{2G}/0_{2C}]$	1608.78	158.28	3.1066	0.1912
2	0.5995	0.4335	$[0_{3C}/0_{3G}/0_{2C}]$	1637.04	141.07	3.1965	0.3026
3	0.5818	0.4162	$[0]_{8C}$	1605.15	197.85	3.0062	0.0000
4	0.5857	0.4885	$[0_{5C}/0_G/0_{2C}]$	1605.04	178.65	3.0897	0.1065
5	0.5870	0.5110	$[0_{3C}/0_{3G}/0_{2C}]$	1601.59	138.22	3.2720	0.3431

Table 11. Optimal results for carbon and S-2 glass fibre reinforced unidirectional hybrid composite with minimum flexural strength 1600 MPa.

	V_{fc}	V_{fg}	Layup (ply 8 – ply 1)	Flexural strength (MPa)	Cost ($\$/m^2$)	Weight (mg/mm^2)	Hybrid ratio
1	0.5006	0.5784	$[0_{2G}/0_{6C}]$	1603.14	168.56	3.1093	0.2780
2	0.5016	0.5784	$[0_{2G}/0_{3C}/0_G/0_{2C}]$	1600.24	164.22	3.2195	0.4089
3	0.5983	0.4797	$[0_{2G}/0_{2C}]_2$	1600.08	164.17	3.2620	0.4450
4	0.5029	0.5784	$[0_{2G}/0_{2C}]_2$	1601.45	159.86	3.3294	0.5349

When the required flexural strength is 1300 MPa, the optimal results are shown in Tables 8 and 9. For both the carbon/E glass and carbon/S-2 glass fibre reinforced hybrid composites, the outermost plies on both the tensile side (ply 1) and compressive side (ply 8) are dominantly carbon/epoxy, except for candidate 3 of the carbon/E glass hybrid composite, which has glass/epoxy plies on both the tensile and compressive sides, and it can also be noticed that its layup is symmetric.

When the required flexural strength is 1600 MPa, the optimal results are shown in Tables 10 and 11. It can be noticed that for the carbon/E glass fibre reinforced hybrid composite, the outermost plies on both the tensile side (ply 1) and compressive side (ply 8) are carbon/epoxy. For S-2 glass fibre, it is more favourable to place glass fibre on the compressive side.

3.2 Multi-directional Hybrid Composites

The NSGA-II-based optimisation converges after 564-1557 runs. The Pareto fronts from NSGA-II optimisation for carbon/E glass fibre reinforced and carbon/S-2 glass fibre reinforced multi-directional hybrid composites are shown in Fig. 7. It is shown that the carbon/E glass fibre reinforced hybrid composite offers lower material cost but higher weight. The carbon/E glass fibre reinforced hybrid composite cannot meet the flexural strength requirement of 900 MPa.

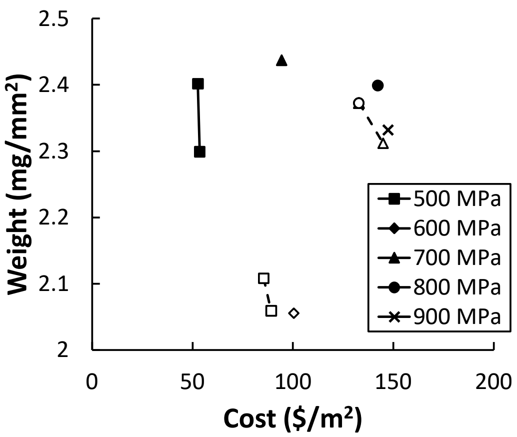

Fig. 7. Pareto fronts from NSGA-II optimisation for carbon and E glass fibre reinforced (filled symbols) and carbon and S-2 glass fibre reinforced multi-directional hybrid composites (open symbols).

Table 12. Optimal results for carbon and E glass fibre reinforced multi-directional hybrid composite.

	V_{fc}	V_{fg}	Layup (ply 8 – ply 1)	Flexural strength (MPa)	Transverse flexural strength (MPa)	Cost ($/m^2)	Weight (mg/mm^2)	Hybrid ratio
500 MPa								
1	0.3191	0.3697	$[(0_2/90/45)_G/(0/90)_C]$	518.28	612.65	53.55	2.2991	0.6985
2	0.3216	0.4379	$[(0_2/90/0)_G/(0/90)_C]$	562.70	619.74	52.66	2.4017	0.7314
700 MPa								
1	0.4785	0.6205	$[90_C/0_G/-45_C/90_G/(90/0)_C]$	863.28	790.92	94.34	2.4370	0.3933
800 MPa								
1	0.6699	0.4546	$[0_C/45_G/(90/45/0/90)_C]$	826.53	1007.37	142.22	2.3989	0.1195

Table 13. Optimal results for carbon and S-2 glass fibre reinforced multi-directional hybrid composite.

	V_{fc}	V_{fg}	Layup (ply 8 – ply 1)	Flexural strength (MPa)	Transverse flexural strength (MPa)	Cost ($/m^2)	Weight (mg/mm^2)	Hybrid ratio
500 MPa								
1	0.3058	0.3019	$[0_C/90_{2G}/0_{2C}/90_G]$	552.10	514.20	85.43	2.1081	0.4969
2	0.3055	0.3024	$[0_C/(90/-45)_G/(45/0/90)_C]$	564.79	539.70	89.14	2.0590	0.3311
600 MPa								
1	0.3524	0.3143	$[(0/45/0)_C/0_G/(0/90)_C]$	638.73	620.46	100.43	2.0554	0.1513
700 MPa								
1	0.6119	0.4423	$[(0/45)_C/(90/45/)_G/(0/90)_C]$	810.33	897.23	132.84	2.3724	0.2655
2	0.6119	0.4423	$[(0/45)_C/(90/0)_G/(0/90)_C]$	835.51	896.00	132.84	2.3724	0.2655
3	0.6348	0.3310	$[(0/-45)_C/45_G/(0_2/90)_C]$	927.42	768.48	144.87	2.3117	0.0944
800 MPa								
1	0.6117	0.4423	$[0_C/(45/90)_G/(45/0/90)_C]$	823.48	827.07	132.82	2.3723	0.1942
1	0.6117	0.4423	$[0_C/(45/90)_G/(0_2/90)_C]$	929.84	822.77	132.82	2.3723	0.1942
900 MPa								
1	0.6468	0.3580	$[(90/0)_C/-45_G/(90_2/0)_C]$	1106.62	945.52	147.27	2.3317	0.0733

The optimal results are shown in Tables 12 and 13, respectively. The hybrid composite mainly contains 0° and 90° plies. The number of carbon/epoxy plies increases with the required flexural strength. Two plies on the tensile face (plies 1 and 2) are carbon/epoxy at 0° and 90°, respectively, or vice versa. The ply angles of the compressive face (ply 6) and tensile face (ply 1) are 0° and 90°, respectively, or vice versa. Interestingly, it is noticed that the plies 2 and 6 have the same ply angle.

4. Conclusions

In this paper, an optimisation study on hybrid composites under flexural loading was presented. One high strength carbon fibre and two types of glass fibres, i.e., S-2 glass and E glass, were chosen to reinforce an epoxy matrix. Both unidirectional and multi-directional hybrid composites were optimised using NSGA-II with minimum cost and weight as the objective functions. It was shown that for a hybrid composite structure, given the load requirement, the layups from the NSGA-II-based optimisation can provide a quantitative selection strategy of carbon and E glass fibres. For the unidirectional hybrid composite, two typical layups can be identified. The first typical layup is placing glass/epoxy plies on the compressive side and carbon/epoxy plies on the tensile side. The second typical layup is placing glass/epoxy plies on the tensile side below the mid-plane. These two typical layups can also be combined. For the multi-directional hybrid composite, no clear rules could be found. The hybrid composite mainly contains about half 0° and half 90° plies. The number of carbon/epoxy plies increases with the required flexural strength. This study carried out an exploratory work for design of lightweight structures. The NSGA-II was coupled with FEA to achieve multi-objective optimisation. This approach can be applied to more complex composite components with load requirements to achieve cost and weight effective optimal designs.

Author Contributions

C. Dong planned the scheme, initiated the project, developed the FEA modelling and code, analysed the results, and prepared the manuscript.

Acknowledgments

Not applicable.

Conflict of Interest

The author declared no potential conflicts of interest concerning the research, authorship, and publication of this article.

Funding

The author received no financial support for the research, authorship, and publication of this article.

Data Availability Statements

The datasets generated and/or analysed during the current study are available from the corresponding author on reasonable request.

References

[1] Dong, C., Ranaweera-Jayawardena, H.A., Davies, I.J., Flexural properties of hybrid composites reinforced by S-2 glass and T700S carbon fibres, *Composites Part B: Engineering*, 43(2), 2012, 573-581.
[2] Dong, C., Duong, J., Davies, I.J., Flexural properties of S-2 glass and TR30S carbon fiber-reinforced epoxy hybrid composites, *Polymer Composites*, 33(5), 2012, 773-781.
[3] Dong, C., Davies, I.J., Flexural properties of glass and carbon fiber reinforced epoxy hybrid composites, *Proceedings of the Institution of Mechanical Engineers, Part L: Journal of Materials Design and Applications*, 227(4), 2013, 308-317.
[4] Dong, C., Sudarisman, Davies, I.J., Flexural properties of E glass and TR50S carbon fiber reinforced epoxy hybrid composites, *Journal of Materials Engineering and Performance*, 22(1), 2013, 41-49.
[5] Papa, I., et al., Carbon/glass hybrid composite laminates in vinylester resin: Bending and low velocity impact tests, *Composite Structures*, 232, 2020, 111571.
[6] Manders, P.W., Bader, M.G., The strength of hybrid glass/carbon fibre composites, *Journal of Materials Science*, 16(8), 1981, 2233-2245.
[7] Rajpurohit, A., et al., Hybrid effect in in-plane loading of carbon/glass fibre based inter- and intraply hybrid composites, *Journal of Composites Science*, 4(1), 2020, 6.
[8] Zhang, C., et al., Low-velocity impact behavior of interlayer/intralayer hybrid composites based on carbon and glass non-crimp fabric, *Materials*, 11(12), 2018, 2472.
[9] Swolfs, Y., Verpoest, I., Gorbatikh, L., Recent advances in fibre-hybrid composites: materials selection, opportunities and applications, *International Materials Reviews*, 64(4), 2019, 181-215.
[10] Ghiasi, H., Pasini, D., Lessard, L., Optimum stacking sequence design of composite materials Part I: Constant stiffness design, *Composite Structures*, 90(1), 2009, 1-11.
[11] Ghiasi, H., et al., Optimum stacking sequence design of composite materials Part II: Variable stiffness design, *Composite Structures*, 93(1), 2010, 1-13.
[12] Nikbakt, S., Kamarian, S., Shakeri, M., A review on optimization of composite structures Part I: Laminated composites, *Composite Structures*, 195, 2018, 158-185.
[13] Sen, P, Yang, J.B., *Multiple Criteria Decision Support in Engineering Design*, Springer, London, 1998.
[14] Hemmatian, H., Fereidoon, A., Assareh, E., Optimization of hybrid laminated composites using the multi-objective gravitational search algorithm (MOGSA), *Engineering Optimization*, 46(9), 2014, 1169-1182.
[15] Hemmatian, H., et al., Optimization of laminate stacking sequence for minimizing weight and cost using elitist ant system optimization, *Advances in Engineering Software*, 57, 2013, 8-18.
[16] Walker, M., Reiss, T., Adali, S., A procedure to select the best material combinations and optimally design hybrid composite plates for minimum weight and cost, *Engineering Optimization*, 29(1-4), 1997, 65-83.
[17] Deb, K., *Multi-Objective Optimization Using Evolutionary Algorithms*, Wiley Interscience Series in Systems and Optimization, Vol. 16, John Wiley & Sons, Chichester, U.K., 2001.
[18] Zitzler, E., Laumanns, M., Thiele, L., *SPEA2: Improving the strength Pareto evolutionary algorithm*, in Tech Rep 103, Computer Engineering and Networks Laboratory (TIK), Swiss Federal Institute of Technology (ETH): Zurich, Switzerland, 2001.
[19] Knowles, J., Corne, D., *The Pareto archived evolution strategy: a new baseline algorithm for Pareto multiobjective optimisation*, in Proceedings of the 1999 Congress on Evolutionary Computation-CEC99 (Cat. No. 99TH8406), 1999.
[20] Deb, K., et al., A fast and elitist multiobjective genetic algorithm: NSGA-II, *IEEE Transactions on Evolutionary Computation*, 6(2), 2002, 182-197.
[21] Kalantari, M., Dong, C., Davies, I.J., Multi-objective robust optimisation of unidirectional carbon/glass fibre reinforced hybrid composites under flexural loading, *Composite Structures*, 138, 2016, 264-275.
[22] Kalantari, M., Dong, C., Davies, I.J., Multi-objective analysis for optimal and robust design of unidirectional glass/carbon fibre reinforced hybrid epoxy composites under flexural loading, *Composites Part B: Engineering*, 84, 2016, 130-139.
[23] Kalantari, M., Dong, C., Davies, I.J., Effect of matrix voids, fibre misalignment and thickness variation on multi-objective robust optimization of carbon/glass fibre-reinforced hybrid composites under flexural loading, *Composites Part B: Engineering*, 123, 2017, 136-147.
[24] Kalantari, M., Dong, C., Davies, I.J., Multi-objective robust optimization of multi-directional carbon/glass fibre-reinforced hybrid composites with manufacture related uncertainties under flexural loading, *Composite Structures*, 182, 2017, 132-142.
[25] Dong, C., Flexural properties of symmetric carbon and glass fibre reinforced hybrid composite laminates, *Composites Part C: Open Access*, 3, 2020, 100047.
[26] Fagan, E.M., et al., Validation of the multi-objective structural optimisation of a composite wind turbine blade, *Composite Structures*, 204, 2018, 567-577.
[27] Bilyeu, B., Brostow, W., Menard, K.P., Epoxy thermosets and their applications I: chemical structures and applications, *Journal of Materials Education*, 21(5/6), 1999, 281-286.
[28] Chou, T.-W., *Microstructural Design of Fiber Composites*, Cambridge University Press, Cambridge, U.K., 1992.
[29] Garnich, M.R., Akula, V.M.K., Review of degradation models for progressive failure analysis of fiber reinforced polymer composites, *Applied Mechanics Reviews*, 62(1), 2008.
[30] ASTM International, Standard Test Method for Flexural Properties of Polymer Matrix Composite Materials, in ASTM D7264/D7264M-15, ASTM International, West Conshohocken, PA, USA, 2015.
[31] Kalantari, M., Dong, C., Davies, I.J., Numerical investigation of the hybridisation mechanism in fibre reinforced hybrid composites subjected to flexural load, *Composites Part B: Engineering*, 102, 2016, 100-111.

ORCID iD

Chensong Dong https://orcid.org/0000-0002-5178-7881

How to cite this article: Dong C. Multi-Objective Optimal Design of Carbon and Glass Reinforced Hybrid Composites under Flexural Loading, *J. Appl. Comput. Mech.*, 8(4), 2022, 1324–1331. https://doi.org/10.22055/jacm.2022.39877.3479